# Stochastic analysis of the effect of spatial variability of diffusion parameters on radionuclide transport in a low permeability clay layer

**Marijke Huysmans · Alain Dassargues**

**Abstract** Most studies that incorporate subsurface heterogeneity in groundwater flow and transport models only analyze and simulate the spatial variability of hydraulic conductivity. Heterogeneity of the other flow and transport parameters are usually neglected. This approach is often justified, but there are, however, cases in which disregarding the heterogeneity of the other flow and transport parameters can be questionable. In low permeability media, for instance, diffusion is often the dominant transport mechanism. It therefore seems logical to incorporate the spatial variability of the diffusion parameters in the transport model. This study therefore analyses and simulates the spatial variability of the effective diffusion coefficient and the diffusion accessible porosity with geostatistical techniques and incorporates their heterogeneity in the transport model of a low permeability formation. The formation studied was Boom clay (Belgium), a candidate host rock for the deep geological disposal of high-level radioactive waste. The calculated output radionuclide fluxes of this model are compared with the fluxes calculated with a homogeneous model and a model with a heterogeneous hydraulic conductivity distribution. This analysis shows that the heterogeneity of the diffusion parameters has a much larger effect on the calculated output radionuclide fluxes than the heterogeneity of hydraulic conductivity in the low permeability medium under study.

Received: 11 February 2005 / Accepted: 28 February 2006
Published online: 24 May 2006



M. Huysmans (✉) · A. Dassargues
KULeuven, Department of Geology-Geography,
Hydrogeology and Engineering Geology Group,
Redingenstraat 16, 3000 Leuven, Belgium
e-mail: marijke.huysmans@geo.kuleuven.ac.be
Tel.: +32-16-326449
Fax: +32-16-326401

A. Dassargues
Hydrogeology and Environmental Geology,
Department of Georesources,
Geotechnologies and Building Materials (GEOMAC),
University of Liège,
B52/3, Liège, Belgium

**Résumé** Analyse stochastique de l'effet de la variation spatiale des paramètres de diffusion sur le transport de radionucléides dans les niveaux argileux de faible perméabilité. La plupart des études qui prennent en compte l'hétérogénéité du sous-sol dans les modèles d'écoulement et de transport de l'eau souterraine analysent et simulent la variation de la conductivité hydraulique. L'hétérogénéité des autres paramètres de l'écoulement et du transport est souvent négligée. Si cette simplification est souvent justifiée, parfois, la non-prise en compte de l'hétérogénéité des autres paramètres de l'écoulement et du transport est discutable. Par exemple, dans les milieux à faible perméabilité, la diffusion est souvent le moyen privilégié de transport. Il paraît par conséquent logique d'incorporer la variabilité de ce paramètre dans le modèle de transport. Cette étude analyse et simule la variation spatiale du coefficient de diffusion et de la porosité disponible pour la diffusion grâce aux techniques géostatistiques. L'hétérogénéité de ces paramètres est prise en compte dans le modèle de transport d'une formation à faible perméabilité. La formation étudiée est celle des argiles de Boom (Belgique), une roche candidate pour l'hébergement à grande profondeur de déchets hautement radioactifs. Les flux sortants de radionucléides nucléides calculés par ce modèle sont comparés aux flux calculés avec un modèle homogène et avec ceux d'un modèle qui intègre une hétérogénéité de la distribution de la conductivité hydraulique. L'analyse montre que dans ce milieu à faible perméabilité, l'hétérogénéité des paramètres de diffusion à des effets bien plus importants sur les flux sortants des radionucléides que l'hétérogénéité de la conductivité hydraulique.

**Resumen** La mayoría de los estudios que incorporan la heterogeneidad subsuperficial en los modelos de flujo y transporte de agua subterránea, sólo analizan y simulan la variabilidad espacial de la conductividad hidráulica. La heterogeneidad de los otros parámetros de flujo y transporte es normalmente menospreciada. Este acercamiento es a menudo justificado, pero sin embargo hay casos en los cuales la falta de atención a la heterogeneidad de los otros parámetros de flujo y de transporte puede ser cuestionable. En los medios de permeabilidad baja, por ejemplo, la difusión es a menudo el mecanismo de transporte dominante. Parece lógico por consiguiente incorporar la variabilidad espacial de los parámetros de difusión en el modelo de transporte. Este estudio analiza

 DOI 10.1007/s10040-006-0035-2

por consiguiente y simula la variabilidad espacial del coeficiente de difusión eficaz y la porosidad de difusión accesible, usando técnicas geoestadisticas e incorpora su heterogeneidad en el modelo de transporte de una formación de permeabilidad baja. La formación estudiada fue la Arcilla Boom (Bélgica), una roca huésped escogida para la disposición geológica profunda de desechos de alto nivel de radiactividad. Los flujos calculados de salida del isótopo radioactivo de este modelo, se comparan con los flujos calculados con un modelo homogéneo y un modelo con una distribución de conductividad hidráulica heterogénea. Este análisis muestra que la heterogeneidad de los parámetros de difusión, tiene un efecto mucho más grande sobre el flujo calculado de salida del isótopo radioactivo, que la heterogeneidad de la conductividad hidráulica en el medio de permeabilidad baja estudiado.

**Keywords** Diffusion · Geostatistics · Waste disposal · Radionuclide transport · Heterogeneity

## Introduction

It is generally recognized that subsurface heterogeneity may have a large influence on groundwater flow and transport of contaminants. Therefore, a large number of recent studies incorporate the underground heterogeneity in hydrogeological flow and transport models using geostatistical techniques (e.g. Scheibe et al. 2001; Copty and Findikakis 2000; Pohlmann et al. 2000). These studies usually only analyze and simulate the spatial variability of hydraulic conductivity, thereby neglecting the heterogeneity of the other flow and transport parameters. This approach is often justified, since advection is usually the dominant transport process. There are, however, cases in which disregarding the heterogeneity of the other flow and transport parameters is questionable. In low permeability media, for instance, diffusion is often the dominant transport mechanism. The effect of transport by advection in such media can be relatively small compared to the effect of transport by diffusion. It therefore seems logical to incorporate the spatial variability of the diffusion parameters in the hydrogeological transport model. The main diffusion parameters are the effective diffusion coefficient and the diffusion accessible porosity as the diffusive mass flux in porous media is given by:

$$F = -\eta D_e \mathrm{grad} C \qquad (1)$$

where $F$ is the diffusive mass flux (kg m$^{-2}$ s$^{-1}$), $\eta$ is the diffusion accessible porosity (–), $D_e$ is the effective diffusion coefficient (m$^2$/s) and $C$ is the solute concentration (kg/m$^3$). The diffusion accessible porosity is not always equal to the total porosity but may be smaller. Only a fraction of the total water-filled porosity is available for diffusive transport. This is caused by size-exclusion effects, i.e. some pores are narrower than the ion size, and by the permanent structural negative charge on the clay surface, which can cause negatively charged ions to be excluded from the narrower interparticle spaces of the clay (Horseman et al. 1996). This study analyses and simulates the spatial variability of the two diffusion parameters and incorporates their heterogeneity in the transport model of a low permeability formation.

The formation studied is the Boom clay in Belgium. This low permeability clay layer is a candidate host rock for the deep geological disposal of high-level radioactive waste. In previous studies, the fate of radionuclides released from a potential repository in the Boom clay was calculated under different assumptions. Mallants et al. (2001) examined radionuclide migration from the vitrified waste through the Boom clay into the surrounding aquifers, assuming that the clay layer was homogeneous. These calculations showed that the magnitude of the fluxes released into the surrounding aquifers was strongly limited by the Boom clay, so that the dose rates were hundreds of times lower than the internationally recommended dose limit. In a later study (Huysmans and Dassargues 2005), the effect of fractures and the spatial variability of hydraulic conductivity were investigated. The output fluxes of this heterogeneous model differed, at most, 8% from the fluxes of the homogeneous model. In the present study, the effect of the spatial variability of the diffusion parameters of the Boom clay is examined. A large number of equally probable random realizations of the clay layer are generated with stochastic simulation and co-simulation procedures using all available hard and soft data. Each of these equiprobable fields is used as input for a transport model that calculates radionuclide transport by advection, diffusion, dispersion, adsorption and decay through the heterogeneous medium. Radionuclide fluxes at the clay-aquifer interfaces are calculated, taking the heterogeneity of the effective diffusion coefficient and the diffusion accessible porosity into account. Radionuclide fluxes computed with this model are compared with fluxes obtained from the previous models.

## Methodology

### Study site

The research activities of the Belgian nuclear repository program, conducted by ONDRAF/NIRAS (Belgian agency for radioactive waste and enriched fissile materials) are concentrated at SCK-CEN (Belgian Nuclear Research Centre) located in the nuclear zone of Mol/Dessel (province of Antwerp). An underground experimental facility (HADES-URF) was built in the Boom clay at 223 m depth. In this area, the Boom clay has a thickness of about 100 m and is overlain by 180 m of water bearing sand formations (Fig. 1). The Boom clay has in this area a vertical hydraulic conductivity of approximately $2\times10^{-12}$ m/s, while the surrounding aquifers have hydraulic conductivity of approximately $2\times10^{-8}$ m/s (Wemaere et al. 2002).

 DOI 10.1007/s10040-006-0035-2

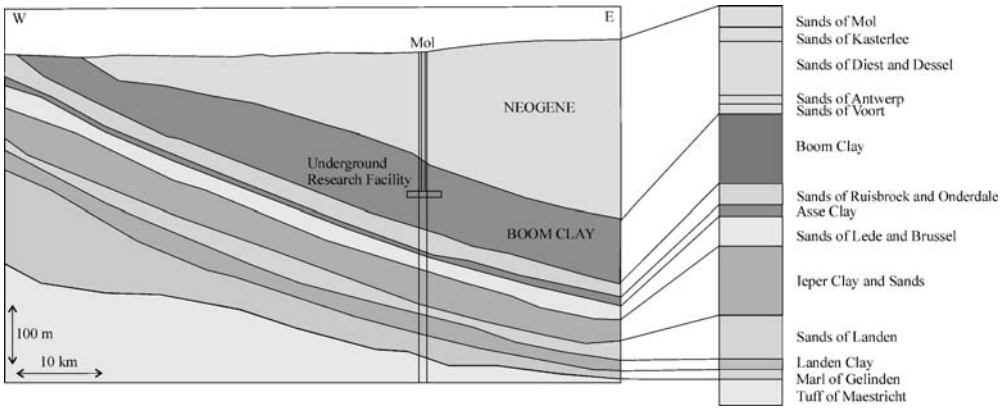


**Fig. 1** Schematic view of Boom clay and location of underground research facility (modified from Mallants et al. 2001). Borehole Mol-1 is located next to the research facility to a depth of 570 m below ground level

## Data set

On the Mol/Dessel site, a 570-m-deep borehole (Mol-1 borehole) was drilled. Several transport and geological parameters (hydraulic conductivity $K$, effective diffusion coefficient $D_e$ and diffusion accessible porosity $\eta$, grain size) have been intensively measured in the laboratory on cores taken at the Mol-1 borehole. Geophysical logging was also performed in the same borehole to obtain logs of gamma ray, resistivity and nuclear magnetic resonance. The resulting data set comprises 41 diffusion coefficient and diffusion-accessible porosity measurements (Fig. 2), 52 hydraulic conductivity values, a gamma ray log, an electrical resistivity log, 71 grain-size measurements (Fig. 3) and a porosity log estimated from the nuclear magnetic resonance log (Fig. 4). Grain size is expressed by the parameter $d_{40}$, the grain size for which 40% of the total sample has a smaller grain size. The diffusion coefficient, hydraulic conductivity, electrical resistivity and grain size show higher values in the lower part of the Boom clay while gamma ray shows lower values in that part. These higher parameter values are all related to the higher grain size in the lower part of the Boom clay (Belsele-Waas Member), which is an indication of sedimentary deposition in a shallower marine environment compared to the middle part of the Boom clay. Diffusion-accessible porosity and nuclear-magnetic-resonance porosity do not show this trend.

## Statistical data analysis

Figure 5 shows the histograms of 41 measurements of the diffusion coefficient $D_e$ and the diffusion accessible

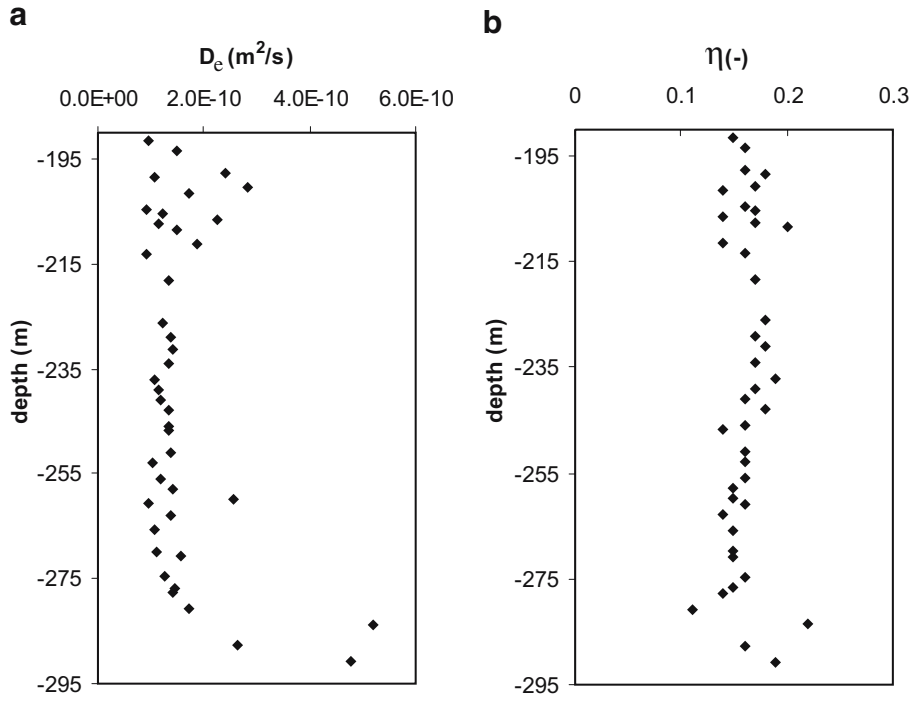


**Fig. 2** **a** Diffusion coefficient $D_e$ (m$^2$/s) and **b** diffusion accessible porosity $\eta$ (–) of iodide in the Boom clay (Aertsens et al. 2004)

 DOI 10.1007/s10040-006-0035-2

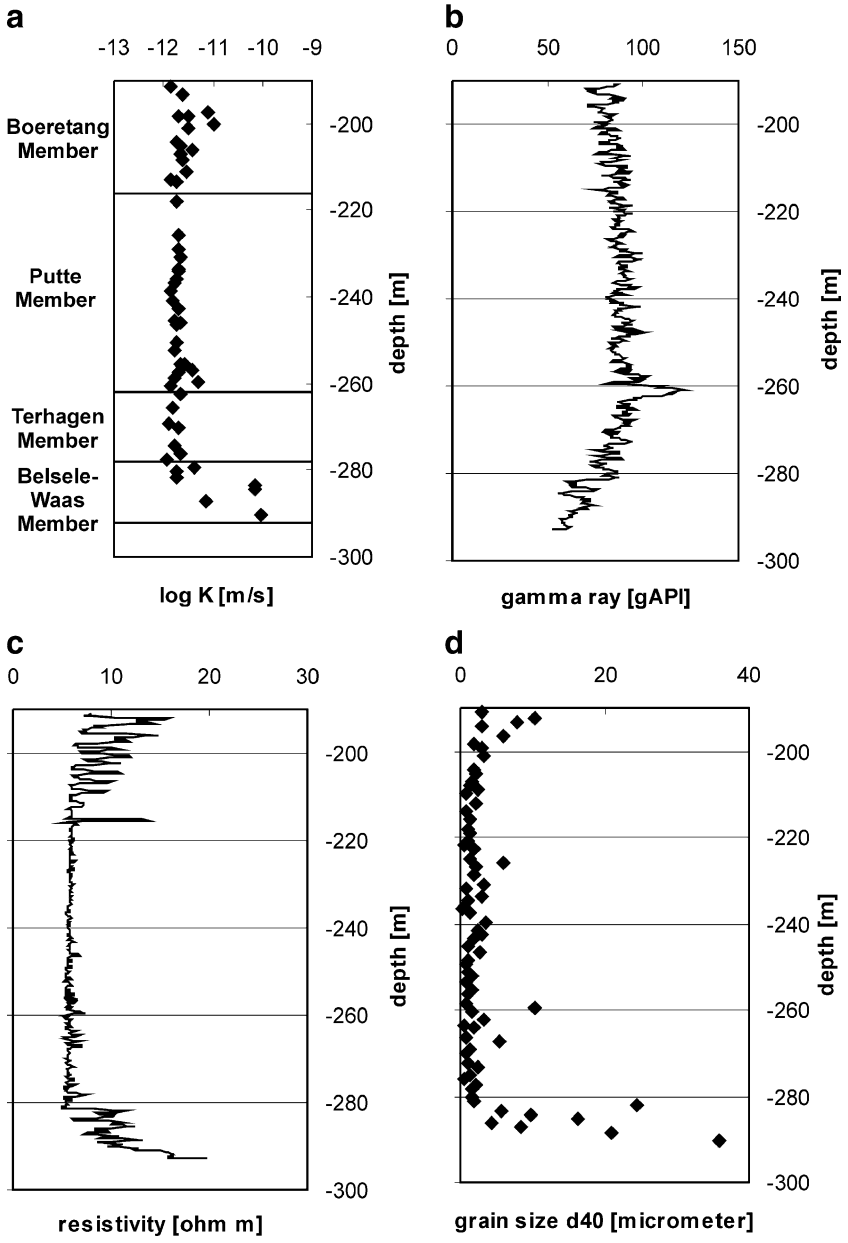


**Fig. 3** **a** Hydraulic conductivity, **b** gamma ray, **c** resistivity and **d** grain size $d_{40}$ of the Boom clay in the Mol-1 borehole (Wemaere et al. 2002)

porosity $\eta$ of iodide in the Boom Clay. The diffusion accessible porosity has a symmetric distribution while the diffusion coefficient shows a skewed distribution. The diffusion accessible porosity has an average value of 0.16 and a standard deviation of 0.02. The minimum and maximum values are 0.11 and 0.22 respectively. The diffusion coefficient $D_e$ has an average value of $1.62\times 10^{-10}$ $m^2/s$ and a standard deviation of $9.03\times10^{-11}$ $m^2/s$. The minimum and maximum values are $9.10\times10^{-11}$ $m^2/s$ and $5.18\times10^{-10}$ $m^2/s$ respectively.

The correlation coefficients of $\eta$ and $D_e$ with the secondary variables are shown in Table 1. Diffusion accessible porosity shows very little correlation with the other variables. The diffusion coefficient, on the contrary, shows a good correlation with hydraulic conductivity, grain size, resistivity and gamma ray.

## Geostatistical data analysis

Geostatistics provides a set of tools to describe the spatial continuity that is an essential feature of many natural phenomena. Definitions of geostatistical estimators are covered extensively by Isaaks and Srivastava (1989) and Deutsch and Journel (1998). The most familiar geostatistical estimator is the semivariogram. The semivariogram, or simply the variogram, is calculated as half of the

 DOI 10.1007/s10040-006-0035-2

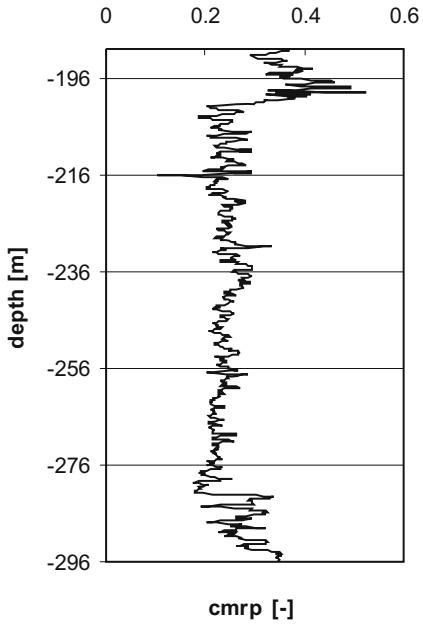


**Fig. 4** Nuclear magnetic resonance porosity CMRP (–) of the Boom clay in the Mol-1 borehole

average squared difference between variable values separated by a lag vector **h**:

$$\gamma_{ii}(\mathbf{h}) = \frac{1}{2N(\mathbf{h})}\sum_{\alpha=1}^{N(\mathbf{h})}\left[z_i(\mathbf{x}_\alpha + \mathbf{h}) - z_i(\mathbf{x}_\alpha)\right]^2 \quad (2)$$

where $\gamma_{ii}(\mathbf{h})$ is the semivariogram, $N(\mathbf{h})$ is the number of pairs, $\alpha$ is a dummy variable and $z_i(\mathbf{x})$ is a regionalized variable. The semivariogram can be understood as the sample variance described as a function of spatial separation. Low semivariogram values indicate a high degree of correlation between variable values separated by the lag vector, while high semivariogram values indicate a low degree of correlation.

The cross-semivariogram, or cross-variogram, is a measure of cross variability between two different variables:

$$\gamma_{ij}(\mathbf{h}) = \frac{1}{2N(\mathbf{h})}\sum_{\alpha=1}^{N(\mathbf{h})}\left[z_i(\mathbf{x}_\alpha + \mathbf{h}) - z_i(\mathbf{x}_\alpha)\right]\left[z_j(\mathbf{x}_\alpha + \mathbf{h}) - z_j(\mathbf{x}_\alpha)\right] \quad (3)$$

where $z_i(\mathbf{x})$ and $z_j(\mathbf{x})$ are regionalized variables.

Variograms and cross-variograms are usually modelled with a variogram model. The model used in this study is the sum of a nugget model and a spherical model:

$$\gamma_{sph}(\mathbf{h}) = \begin{cases} 0 & \text{if } |\mathbf{h}| = a \\ C_0 + C\left[1.5\frac{|\mathbf{h}|}{a} - 0.5\left(\frac{|\mathbf{h}|}{a}\right)^3\right] & \text{otherwise} \\ C_0 + C & \text{if } |\mathbf{h}| > a. \end{cases} \quad (4)$$

where $C_0$ is the nugget effect, $C$ is the sill and $a$ is the range.

Since diffusion accessible porosity shows no correlation with the other variables, only a variogram is calculated and fitted. Figure 6 shows the experimental and fitted diffusion accessible porosity variogram. It is fitted with the sum of a nugget model of 0.00015 and a spherical model with a range of 5.8 m and a sill of 0.00018. The small range and the relatively large nugget effect suggest that this variable shows little spatial correlation.

The diffusion coefficient $D_e$ shows a strong correlation with all secondary variables. These secondary variables are therefore all incorporated in the simulation procedure. Therefore, it is necessary to calculate variograms of each variable and cross-variograms of each combination of two variables. The dots in Fig. 7 represent the experimental

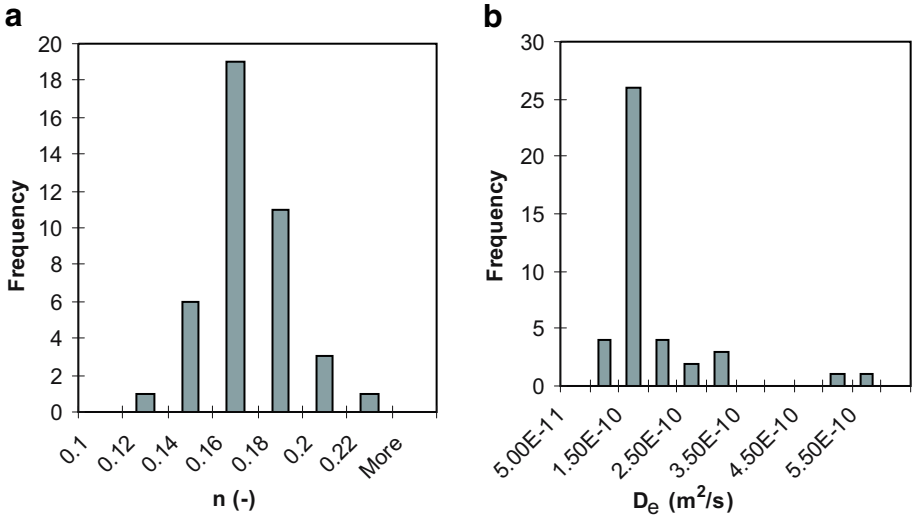


**Fig. 5** Histograms of **a** diffusion coefficient $D_e$ ($m^2/s$) and **b** diffusion accessible porosity $\eta$ (–) of iodide in the Boom clay

 DOI 10.1007/s10040-006-0035-2

**Table 1** Correlation coefficients of the diffusion coefficient and the diffusion accessible porosity with secondary variables

| | $\eta$ (–) | $D_e$ ($m^2$/s) |
|---|---|---|
| $Log_{10}$ hydraulic conductivity (m/s) | 0.44 | 0.97 |
| Gamma ray (ohm m) | –0.20 | –0.63 |
| Resistivity (gAPI) | 0.20 | 0.66 |
| Grain size $d_{40}$ (μm) | 0.28 | 0.93 |
| Porosity CMRP[a] (–) | 0.31 | 0.20 |

[a] CMRP is the nuclear magnetic resonance porosity

variograms and cross-variograms of all variables, calculated in 25 lags with a lag distance of 3 m. The shape of most variograms suggests fitting by a spherical model. The average range is approximately 35 m.

Modelling the variograms and cross-variograms of two or more variables is more complicated than modelling the variogram of a single variable. The variograms and cross-variograms must satisfy certain conditions to ensure that estimates derived from cokriging (i.e. a geostatistical spatial interpolation method) have a positive or zero variance. The linear model of coregionalization provides a method for modelling the variograms and cross-variograms of two or more variables so that the variance of any possible linear combination of these variables is always positive (Isaaks and Srivastava 1989). Each variogram and cross-variogram is represented as a sum of the same elementary variogram models $[\gamma_u(\mathbf{h}), = 0, \ldots, S]$:

$$\gamma_{ij}(\mathbf{h}) = \sum_{u=0}^{S} b_{ij}^{u} \gamma_u(\mathbf{h}) \tag{5}$$

where $S+1$ is the number of structures and $b_{ij}$ are symmetric coefficients that define a positive definite matrix $B=(b_{ij})$. A necessary, but not sufficient, condition for the coefficients is

$$\left| b_{ij}^{u} \right| \leq \sqrt{b_{ii}^{u} b_{jj}^{u}} \tag{6}$$

which implies that every elementary structure present in the cross-variogram of the ith and jth variables must also be present in the ith and jth variograms. However, a structure that appears on a variogram is not necessarily present on the cross-variogram for that variable (Pardo-Iguzquiza and Dowd 2002).

In this study, variograms and cross-variograms of $D_e$ and all secondary variables are modelled as the sum of a nugget model and a spherical model with a range of 35 m. The sills are fitted by the optimization program LCMFIT2 (Pardo-Iguzquiza and Dowd 2002). Figure 7 shows the fitted variograms and cross-variograms of all variables.

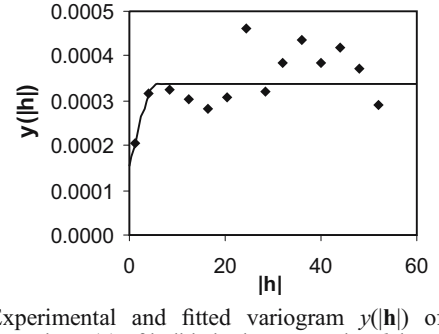


**Fig. 6** Experimental and fitted variogram $y(|\mathbf{h}|)$ of diffusion accessible porosity $\eta$ (–) of iodide in the Boom clay. $h$ lag distance (m)

## Simulation of the diffusion coefficient and the diffusion accessible porosity

The real spatial distributions of the diffusion coefficient and the diffusion accessible porosity of the Boom clay are not completely known. Therefore, a large number of equally probable random realizations of the clay layer are generated, using the modelled variograms and cross-variograms. Realizations of the diffusion coefficient are generated using measurements of the diffusion coefficient, hydraulic conductivity, gamma ray, resistivity and grain size measurements. Realizations of the diffusion accessible porosity are generated using measurements of the diffusion accessible porosity only. The realizations honour the measured data and the mean, variance and variogram of both diffusion parameters.

The Boom clay shows a lateral continuity that largely exceeds the extent of the local scale model (Wouters and Vandenberghe 1994). Therefore, it is assumed that the properties of the Boom clay do not vary in the horizontal direction and one-dimensional vertical realizations of the diffusion accessible porosity and the diffusion coefficient were generated.

The diffusion coefficient and the diffusion accessible porosity for iodide are simulated with direct sequential simulation with histogram reproduction. The simulation algorithm is iterative and contains the following steps:

1. The location to be simulated is randomly chosen along the vertical axis. The spacing between the locations to be simulated is 0.2 m.
2. The simple cokriging estimate and variance are calculated using the original primary and secondary data and all previously simulated values using COKB3D (Deutsch and Journel 1998).
3. The shape of the local hydraulic-conductivity distribution in each location is determined in such a way that the original histogram of hydraulic conductivity is reproduced by the simulation. This is achieved by the following approach (Oz et al. 2003). Before the start of the simulation, a look-up table is constructed by generating non-standard Gaussian distributions by choosing regularly spaced mean values (approximately from –3.5 to 3.5) and variance values (approximately from 0 to 2). The distribution of uncertainty in the data space can then be determined from back transformations of these non-standard univariate Gaussian

 DOI 10.1007/s10040-006-0035-2

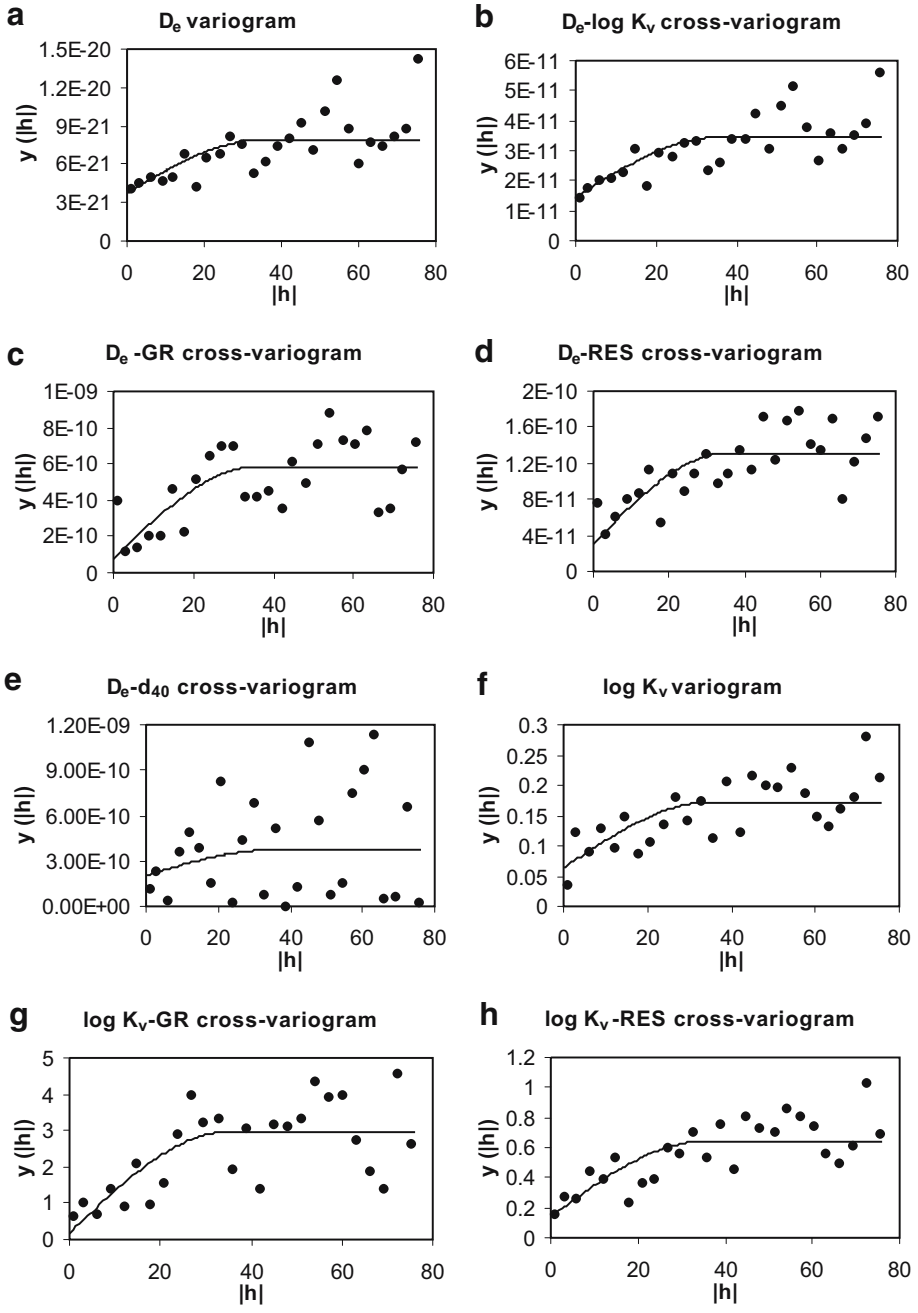


**Fig. 7** Experimental **a** variogram of $D_e$, **b** cross-variogram of $D_e$ and log $K_v$, **c** cross-variogram of $D_e$ and GR, **d** cross-variogram of $D_e$ and RES, **e** cross-variogram of $D_e$ and $d_{40}$, **f** variogram of log $K_v$, **g** cross-variogram of log $K_v$ and GR and **h** cross-variogram of log $K_v$ and RES, all fitted with a linear coregionalization model—*h* lag distance (m), $D_e$ diffusion coefficient ($m^2$/s) of iodide, $K_v$ vertical hydraulic conductivity (m/s), GR gamma ray (ohm m), *RES* Resistivity (gAPI), $d_{40}$ grain size (μm). Experimental **i** cross-variogram of log $K_v$ and $d_{40}$, **j** variogram of GR, **k** cross-variogram of GR and RES, **l** cross-variogram of GR and $d_{40}$, **m** variogram of RES, **n** cross-variogram of RES and $d_{40}$ and (**o**) variogram of $d_{40}$, all fitted with a linear coregionalization model (*h* lag distance in metres), $D_e$ diffusion coefficient ($m^2$/s) of iodide, $K_v$ vertical hydraulic conductivity (m/s), *GR* gamma ray (ohm m), *RES* resistivity (gAPI), $d_{40}$ grain size (μm)

distributions by back transformation of $L$ regularly spaced quantiles, $p^l$, $l=1,...,L$:

$$K^l = F_K^{-1}\left\{G\left[G^{-1}\left(p^l\right)\sigma_y + y^*\right]\right\}, \quad l = 1, ..., L \qquad (7)$$

where $F_K(K)$ is the cumulative distribution function from the original $K$ variable, $G(y)$ is the standard normal cumulative distribution function, $y^*$ and $\sigma_y$ are the mean and standard deviation of the non-standard Gaussian distribution and the $p^l$, $l=1,...,L$ are uniformly distributed values between 0 and 1. From this look-up table, the closest $K$-conditional distribution is retrieved by searching for the one with the closest mean and variance to the cokriging values (Oz et al. 2003).

 DOI 10.1007/s10040-006-0035-2

**Fig. 7** (continued)

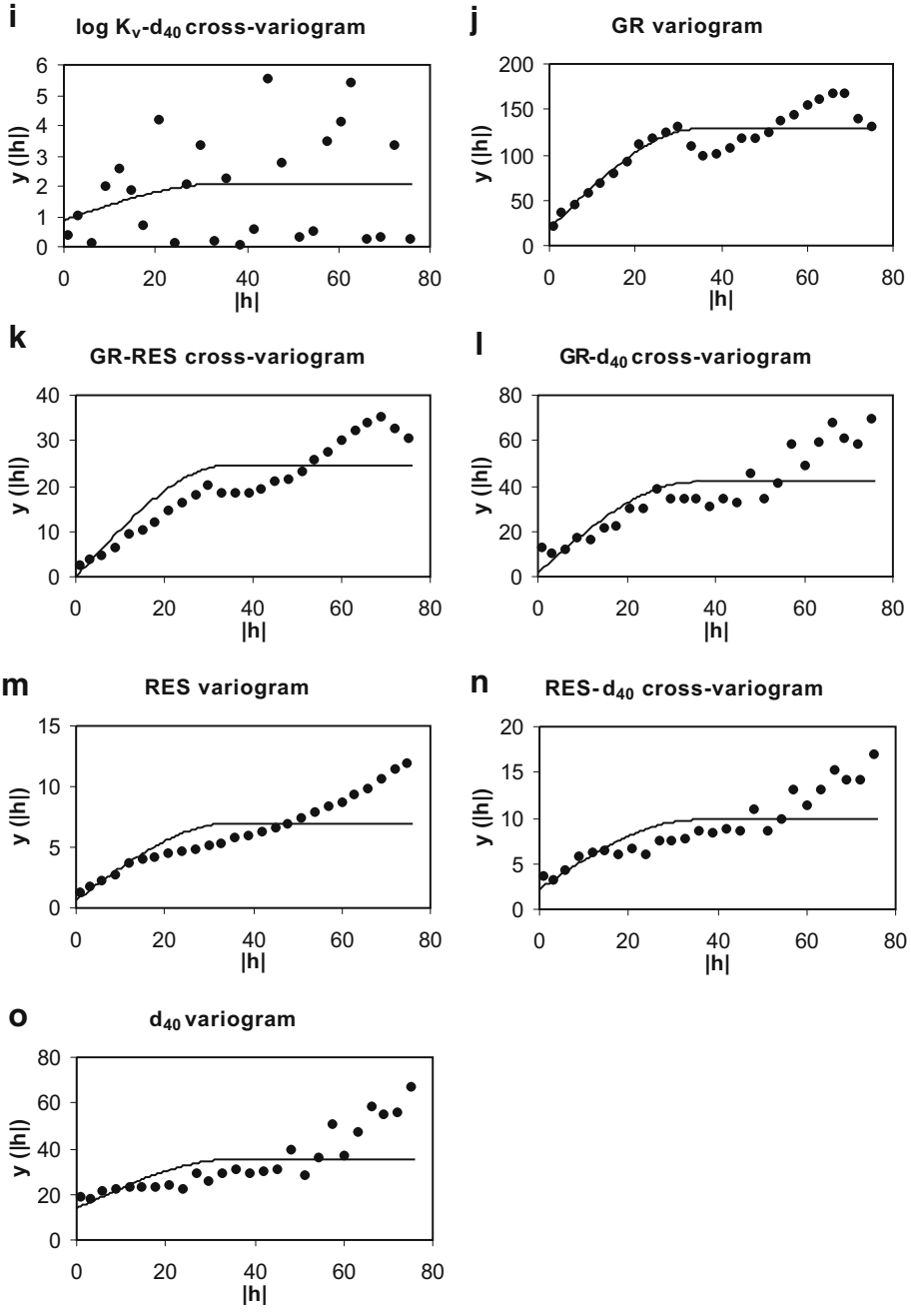


4. A value is drawn from the *K*-conditional distribution by Monte-Carlo simulation and assigned to the location to be simulated.

This approach creates realizations that reproduce the (1) local point and block data in the original data units, (2) the mean, variance and variogram of the variable and (3) the histogram of the variable (Oz et al. 2003). Figure 8 shows one simulation of diffusion accessible porosity and one simulation of the diffusion coefficient of iodide. The simulation of the diffusion accessible porosity reflects the symmetric distribution of $\eta$, while the simulation of the diffusion coefficient shows a skewed distribution. The simulated diffusion accessible porosity shows no trend, whereas the simulated diffusion coefficient has higher values in the lower part of the Boom clay, which is caused by conditioning to measurements of the diffusion coefficient and the secondary variables.

## Local three-dimensional hydrogeological model

A local three-dimensional hydrogeological groundwater flow and transport model of the Boom clay is constructed. The clay is conceptualized as a porous medium with

 DOI 10.1007/s10040-006-0035-2

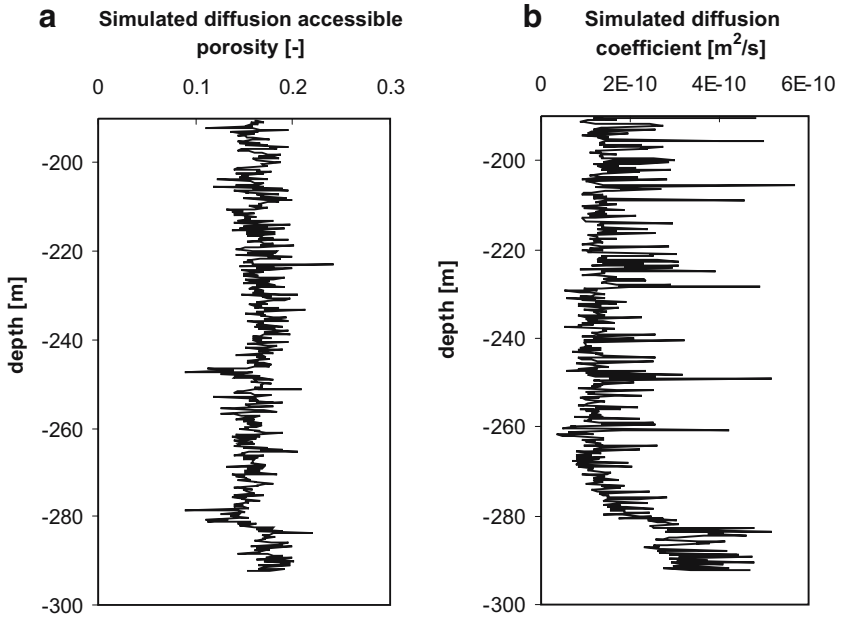


**Fig. 8** **a** Simulation of diffusion accessible porosity $\eta$ (–) and **b** simulation of diffusion coefficient $D_e$ ($m^2/s$)

spatially varying diffusion parameters in the vertical direction. Flow is considered to be one-dimensional vertical and stationary. A radionuclide source is assumed to be located in the middle of the clay layer. The transport processes taken into account are advection, dispersion, molecular diffusion and radioactive decay.

The model width in the *x*-direction is 20 m, i.e. half the distance between the disposal galleries. The model length in the *y*-direction is 15 m. The model dimension in the *z*-direction is 102 m, i.e. the total thickness of the Boom clay in the nuclear zone of Mol-Dessel. The grid spacing is 1m in the *x*-direction and in the *y*-direction and varies between 0.2 m and 1 m in the *z*-direction. The horizontal and vertical hydraulic conductivity are $7\times10^{-12}$ m/s and $2.8\times10^{-12}$ m/s respectively. The vertical boundary conditions for groundwater flow are zero flux boundary conditions since the hydraulic gradient is vertical. The horizontal boundary conditions for groundwater flow are Dirichlet conditions. The specified head at the upper boundary is 2 m higher than the specified head at the lower boundary since the downward vertical hydraulic gradient is approximately 0.02 in the 100-m-thick Boom clay (Wemaere and Marivoet 1995).

Transport by advection, dispersion, molecular diffusion and radioactive decay is calculated for three radionuclides: $^{79}$Se, $^{129}$I and $^{99}$Tc. Previous calculations revealed that they were the most important in terms of dose rates from a potential high-level waste repository for vitrified waste (Mallants et al. 1999). The properties of these radionuclides are given in Table 2. The boundary conditions for transport at the upper and lower boundaries are zero concentration boundary conditions (Mallants et al. 1999), since the hydraulic conductivity contrast between the clay and the aquifer is so large that solutes reaching the boundaries are assumed to be flushed away by advection in the aquifer. The source term models for the three radionuclides are as described by Mallants et al. 1999. The radionuclides are contained in borosilicate glass and as the glass corrodes, the radionuclides become available for dissolution into the groundwater. A constant glass dissolution rate of 3 μm/year is assumed. Since the initial radius of the cylindrical glass matrix would be 0.215 m, the glass matrix would be completely dissolved after approximately 70,000 years. The source term model is therefore a constant flux over a period of 70,000 years equal to the total radionuclide inventory divided by 70,000 years, i.e., $8.51\times10^{6}$ Bq/year for $^{129}$I, $9.30\times10^{8}$ Bq/year for $^{79}$Se and $3.94\times10^{10}$ Bq/year for $^{99}$Tc, where the becquerel (Bq) is the unit of radioactivity, defined as the activity of a quantity of radioactive material in which one nucleus decays per second. If, however, this source term model resulted in calculated concentrations higher than the solubility limit, which is the case for $^{79}$Se and $^{99}$Tc, the source term model was replaced by a constant concentration model. A constant concentration equal to the solubility limit was then prescribed until exhaustion of the source.

For the radionuclide $^{129}$I, the different equiprobable realizations of the diffusion coefficient and diffusion accessible porosity of iodide are directly imported in the model. For $^{79}$Se and $^{99}$Tc, previous studies indicate that

**Table 2** Properties of selected radionuclides (from Mallants et al. 1999). $^{129}$I reaches no solubility limit in Boom clay porewater

| | $^{79}$Se | $^{129}$I | $^{99}$Tc |
|---|---|---|---|
| Half-life (year) | $6.50\times10^{4}$ | $1.57\times10^{7}$ | $2.13\times10^{5}$ |
| Decay constant ($year^{-1}$) | $1.07\times10^{-5}$ | $4.41\times10^{-8}$ | $3.25\times10^{-6}$ |
| Solubility limit (mole/l) | $5.5\times10^{-8}$ | – | $3\times10^{-8}$ |
| Retardation factor (–) | 1 | 1 | 1 |

 DOI 10.1007/s10040-006-0035-2

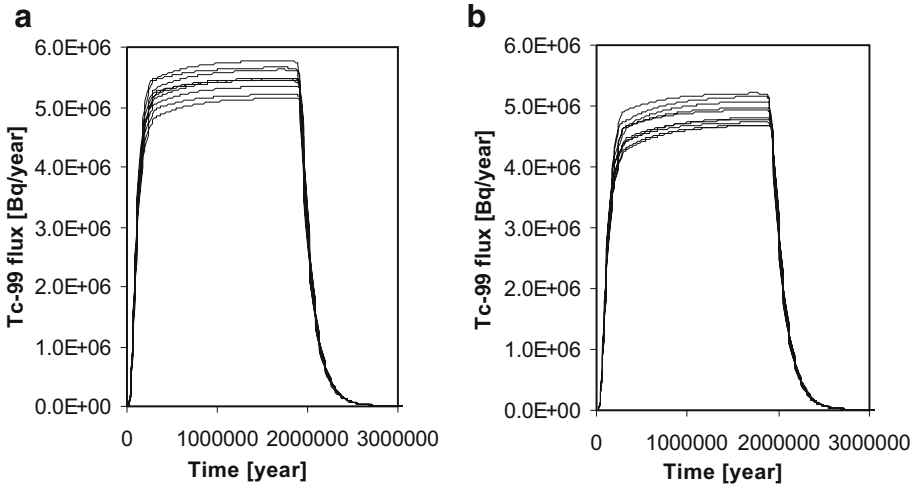


**Fig. 9** Total $^{99}$Tc fluxes through **a** the lower clay-aquifer interface and **b** the upper clay-aquifer interface

the diffusion coefficient is approximately equal to the diffusion coefficient of iodide. Therefore, the realizations of the diffusion coefficient were also used to model transport of $^{79}$Se and $^{99}$Tc. The diffusion accessible porosity of these radionuclides is, however, different. While the average value of the diffusion accessible porosity of iodide is 0.16, $^{79}$Se and $^{99}$Tc are reported to have diffusion accessible porosities of 0.13 and 0.30 respectively. Therefore, the simulations of the diffusion accessible porosity of iodide were rescaled for $^{79}$Se and $^{99}$Tc so that the average values of the simulated porosities were equal to 0.13 and 0.30.

This local three-dimensional hydrogeological model was run with FRAC3DVS, a simulator for three-dimensional groundwater flow and solute transport in porous, discretely fractured porous or dual-porosity formations (Therrien and Sudicky 1996; Therrien et al. 2003). This model was run for ten different random combinations of simulations of the diffusion coefficient and the diffusion accessible porosity. Only ten realizations are generated since the results show that the difference between the calculated radionuclide fluxes of the ten different simulations is rather small. The results of this model were compared with the results of a homogeneous model.

## Results

Figure 9 shows the computed total $^{99}$Tc fluxes through the lower and upper clay-aquifer interface for ten different equally probable simulations. The $^{99}$Tc fluxes through the clay-aquifer interfaces increase relatively fast during the first 200,000 years. From 200,000 until 1,750,000 years, the fluxes increase more gradually. The fluxes decrease afterwards due to exhaustion of the source. The difference between the fluxes of the ten different simulations is the largest in the time period from 200,000 until 1,750,000 years. The total amount of $^{99}$Tc leaving the clay was calculated as flux integrated over time for each simulation. The total $^{99}$Tc amounts or activities leaving the clay vary between $9.84\times10^{12}$ Bq and $1.092\times10^{13}$ Bq through the lower clay-aquifer interface and between

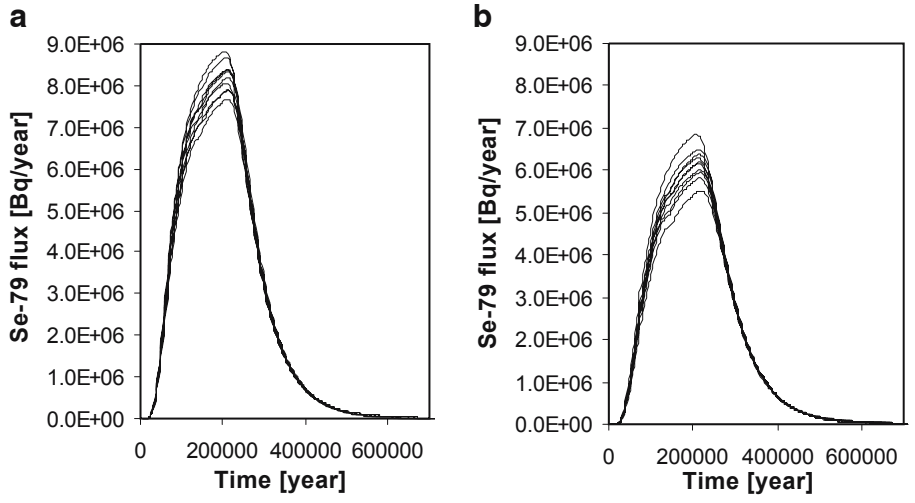


**Fig. 10** Total $^{79}$Se fluxes through **a** the lower clay-aquifer interface and **b** the upper clay-aquifer interface

 DOI 10.1007/s10040-006-0035-2

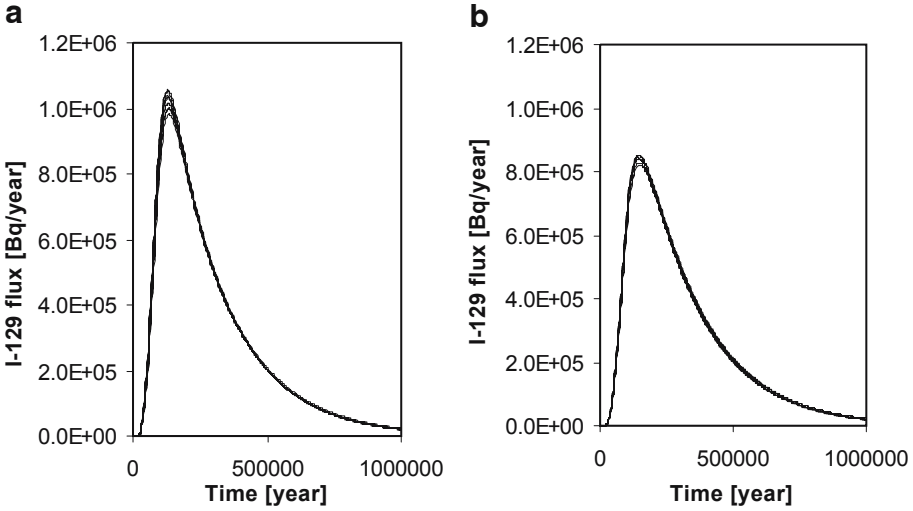


**Fig. 11** Total $^{129}$I fluxes through **a** the lower clay-aquifer interface and **b** the upper clay-aquifer interface

$8.91\times10^{12}$ Bq and $9.86\times10^{12}$ Bq through the upper clay-aquifer interface.

Figure 10 shows the computed total $^{79}$Se fluxes through the lower and upper clay-aquifer interface for the ten different simulations. The $^{79}$Se fluxes through the clay-aquifer interfaces gradually increase until they reach a maximum after approximately 200,000 years and decrease slowly afterwards due to exhaustion of the source. The difference between the fluxes of the ten different simulations is the largest in the time period from 100,000 until 200,000 years. The total $^{79}$Se activities leaving the clay vary between $1.68\times10^{12}$ Bq and $1.88\times10^{12}$ Bq through the lower clay-aquifer interface and between $1.30\times10^{12}$ Bq and $1.49\times10^{12}$ Bq through the upper clay-aquifer interface.

The calculated $^{129}$I fluxes through the lower and upper clay-aquifer interface for ten simulations are shown in Fig. 11. The differences between the fluxes of the different simulations are rather small. The fluxes through the clay-aquifer interfaces increase until they reach a maximum after approximately 120,000 years and decrease slowly afterwards. The total $^{129}$I activities leaving the clay vary between $2.86\times10^{11}$ Bq and $2.99\times10^{11}$ Bq through the lower clay-aquifer interface and between $2.62\times10^{11}$ Bq and $2.74\times10^{11}$ Bq through the upper clay-aquifer interface. The smaller degree of variance in the results for $^{129}$I is caused by its much larger half-life compared to the other radionuclides. For decaying solutes, higher diffusion parameters not only decrease the travel time, but they also decrease the amount of solute that has been decayed before arrival. The smaller the decay constant, the smaller the effect of the diffusion parameters on the solutes fluxes.

In Fig. 12, a comparison is made between the radionuclide activities calculated with the heterogeneous simulations and a homogeneous model with a homogeneous diffusion coefficient and diffusion accessible poros-

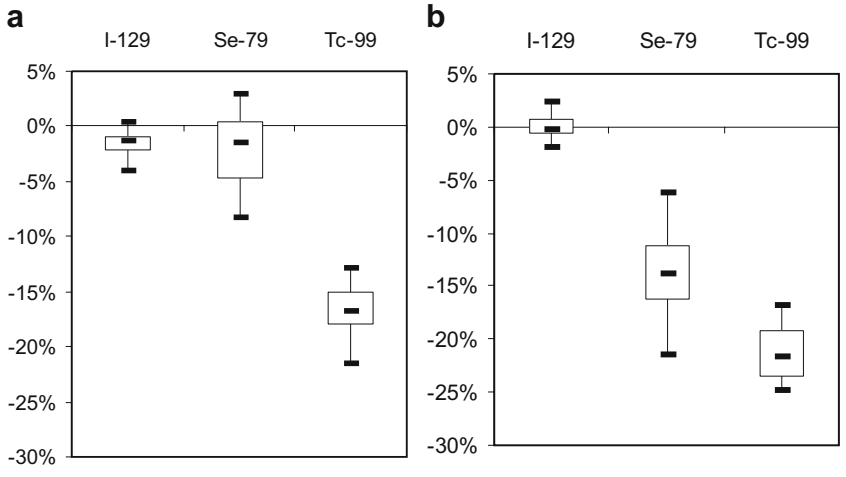


**Fig. 12** Boxplots of difference in percentage of total radionuclide activity between heterogeneous and homogeneous model **a** through the lower clay-aquifer interface and **b** through the upper clay-aquifer interface

 DOI 10.1007/s10040-006-0035-2

ity equal to the average values. The figures show boxplots of the difference in percentage of total radionuclide activity between the heterogeneous and the homogeneous model. Compared to the homogeneous model, the radionuclide activity flowing through the lower clay-aquifer is between 21% smaller and 3% larger in the heterogeneous model. The radionuclide activity flowing through the upper clay-aquifer is between 25% smaller and 2.5% larger.

## Discussion

A model with a heterogeneous diffusion coefficient and diffusion accessible porosity distribution results in fluxes that are up to 25% different from the fluxes calculated with a homogeneous model with a homogeneous diffusion coefficient and diffusion accessible porosity equal to the average values. The output fluxes of a previous model with a heterogeneous hydraulic conductivity distribution differed at most 8% from the fluxes of the homogeneous model (Huysmans and Dassargues 2005). The coefficient of variation, i.e. standard deviation divided by mean value, of hydraulic conductivity is 2.75. This value is much larger than the coefficients of variation of the diffusion coefficient and diffusion accessible porosity, 0.125 and 0.557 respectively. Although hydraulic conductivity shows a much larger relative spatial variability than the diffusion coefficient and the diffusion accessible porosity, the heterogeneity of the diffusion parameters has a much larger effect on the output fluxes than the heterogeneity of hydraulic conductivity. Only incorporating the spatial variability of hydraulic conductivity would thus result in a serious underestimation of the effect of heterogeneity on the output fluxes.

This can be explained by the large importance of transport by diffusion in low permeability media. The effect of transport by advection in such media is usually small compared to the effect of transport by diffusion. The solute concentrations and fluxes are thus much more sensitive to changes in diffusion parameters than to changes in hydraulic conductivity.

## Conclusions

Most studies that incorporate subsurface heterogeneity in groundwater flow and transport models only analyze and simulate the spatial variability of hydraulic conductivity. The heterogeneity of the other flow and transport parameters is usually neglected. This study has shown that this approach is not always justified. Radionuclide transport in a low-permeability clay was simulated, taking the spatial variability of the diffusion coefficient and the diffusion accessible porosity into account. The output fluxes of this model were compared with a homogeneous model and with a model with a heterogeneous hydraulic conductivity distribution. Although hydraulic conductivity has a much larger relative spatial variability than the diffusion coefficient and the diffusion accessible porosity, the heterogeneity of the diffusion parameters proved to have a much larger effect on the output fluxes than the heterogeneity of hydraulic conductivity. This can be explained by the large importance of transport by diffusion in low permeability media. The solute concentrations and fluxes are much more sensitive to changes in diffusion parameters than to changes in hydraulic conductivity.

A hydrogeological study incorporating subsurface heterogeneity should therefore start with a sensitivity analysis of the different flow and transport parameters. The effect of the expected spatial variation in hydraulic conductivity $K$, effective porosity $n_e$, diffusion coefficient $D_e$, diffusion accessible porosity $\eta$, distribution coefficient $K_d$, etc. on the results should be examined. Based on this analysis, a selection should be made of the parameters for which the spatial variability should be incorporated in the model.

**Acknowledgements** The authors wish to acknowledge the Fund for Scientific Research-Flanders for providing a Research Assistant scholarship to the first author. We also wish to thank ONDRAF/NIRAS (Belgium agency for radioactive waste and enriched fissile materials) and SCK-CEN (Belgian Nuclear Research Centre) for providing the necessary data for this study. We also thank René Therrien and Rob McLaren for providing FRAC3DVS and for their assistance. We thank the anonymous reviewers for their constructive reviews.

## References

Aertsens M, Wemaere I, Wouters L (2004) Spatial variability of transport parameters in the Boom Clay. Appl Clay Sci 26(1–4):37–45

Copty NK, Findikakis AN (2000) Quantitative estimates of the uncertainty in the evaluation of ground water remediation schemes. Ground Water 38(1):29–37

Deutsch CV, Journel AG (1998) GSLIB geostatistical software library and user's guide. Oxford University Press, New York

Horseman ST, Higgo JJW, Alexander J, Harrington JF (1996) Water, gas and solute movement through argillaceous media. Nuclear Energy Agency, Organisation for Economic Co-operation and Development, Paris

Huysmans M, Dassargues A (2005) Stochastic analysis of the effect of heterogeneity and fractures on radionuclide transport in a low permeability clay layer. Environ Geol 48(7):920–930

Isaaks EH, Srivastava RM (1989) An introduction to applied geostatistics. Oxford University Press, New York

Mallants D, Sillen X, Marivoet J (1999) Geological disposal of conditioned high-level and long-lived radioactive waste: consequence analysis of the disposal of vitrified high-level waste in the case of the normal evolution scenario, ONDRAF/NIRAS report R-3383, ONDRAF/NIRAS, Brussels, Belgium

Mallants D, Marivoet J, Sillen X (2001) Performance assessment of vitrified high-level waste in a clay layer. J Nucl Mater 298 (1–2):125–135

Oz B, Deutsch CV, Tran TT, Xie Y (2003) DSSIM-HR: A FORTRAN 90 program for direct sequential simulation with histogram reproduction. Comput Geosci 29(1):39–51

Pardo-Iguzquiza E, Dowd PA (2002) FACTOR2D: a computer program for factorial cokriging. Comput Geosci 28(8):857–875

Pohlmann K, Hassan A, Chapman J (2000) Description of hydrogeologic heterogeneity and evaluation of radionuclide transport at an underground nuclear test. J Contam Hydrol 44(3–4): 353–386

 DOI 10.1007/s10040-006-0035-2

Scheibe TD, Chien Y-J, Radtke JS (2001) Use of quantitative models to design microbial transport experiments in a sandy aquifer. Ground Water 39(2):210–222

Therrien R, Sudicky EA (1996) Three-dimensional analysis of variably-saturated flow and solute transport in discretely-fractured porous media. J Contam Hydrol 23(1–2):1–44

Therrien R, Sudicky EA, McLaren RG (2003) FRAC3DVS: An efficient simulator for three-dimensional, saturated-unsaturated groundwater flow and density dependent, chain-decay solute transport in porous, discretely-fractured porous or dual-porosity formations, User's guide, Groundwater Simul. Group, Waterloo, Ontario, Canada

Wemaere I, Marivoet J (1995) Geological disposal of conditioned high-level and long lived radioactive waste: updated regional hydrogeological model for the Mol site (the north-eastern Belgium model), ONDRAF/NIRAS Report R-3060, ONDRAF/NIRAS, Brussels, Belgium

Wemaere I, Marivoet J, Labat S, Beaufays R, Maes T (2002) Mol-1 borehole (April–May 1997): Core manipulations and determination of hydraulic conductivities in the laboratory, ONDRAF/NIRAS Report R-3590, ONDRAF/NIRAS, Brussels, Belgium

Wouters L, Vandenberghe N (1994) Geologie van de Kempen: een synthese, ONDRAF/NIRAS Report NIROND-94-11, ONDRAF/NIRAS, Brussels, Belgium

 DOI 10.1007/s10040-006-0035-2